ORIGINAL PAPER

A Simple QD–FRET Bioprobe for Sensitive and Specific Detection of Hepatitis B Virus DNA

Shan Huang · Hangna Qiu · Qi Xiao · Chusheng Huang · Wei Su · Baoqing Hu

Abstract We report here a simple quantum dot-FRET (QD-FRET) bioprobe based on fluorescence resonance energy transfer (FRET) for the sensitive and specific detection of hepatitis B virus DNA (HBV DNA). The proposed one-pot HBV DNA detection method is very simple, rapid and convenient due to the elimination of the washing and separation steps. In this study, the water-soluble CdSe/ZnS QDs were prepared by replacing the trioctylphosphine oxide on the surface of QDs with mercaptoacetic acid (MAA). Subsequently, DNA was attached to QDs surface to form the functional QD-DNA bioconjugates by simple surface ligand exchange. After adding 6-carboxy-X-rhodamine (ROX)-modified HBV DNA (ROX-DNA) into the QD-DNA bioconjugates solution, DNA hybridization between QD-DNA bioconjugates and ROX-DNA was formed. The resulting hybridization brought the ROX fluorophore, the acceptor, and the QDs, the donor, into proximity, leading to energy transfer from QDs to ROX. When ROX-DNA was displaced by the unlabeled HBV DNA, the efficiency of FRET was dramatically decreased. Based on the changes of both fluorescence intensities of QDs and ROX, HBV DNA could be detected with high sensitivity and specificity. Under the optimized conditions, the linear range of HBV DNA determination was 2.5 – 30 nmol L^{-1}, with a correlation coefficient (R) of 0.9929 and a limit of detection (3σ black) of 1.5 nmol L^{-1}. The relative standard deviation (R.S.D.) for 12 nmol L^{-1} HBV DNA was 0.9 % ($n=5$). There was no interference to non-complementary DNA.

S. Huang · H. Qiu · Q. Xiao · C. Huang · W. Su
College of Chemistry and Life Science, Guangxi Teachers
Education University, Nanning 530001, People's Republic
of China

Q. Xiao (✉) · B. Hu
Key Laboratory of Beibu Gulf Environment Change and
Resources Utilization (Guangxi Teachers Education University),
Ministry of Education, Nanning, People's Republic of China
e-mail: qi.xiao@whu.edu.cn

Time-resolved fluorescence spectra and fluorescence images were performed to verify the validity of this method and the results were satisfying.

Keywords Quantum dots · Hepatitis B virus DNA · Fluorescence resonance energy transfer · Bioprobe

Introduction

During the past two decades, luminescent semiconductor quantum dots (QDs) have attracted widespread attention as novel fluorescence indicator in numerous bio-sensing, bio-analysis and bio-detection [1–3]. Compared to traditional organic dyes and fluorescent proteins, QDs have some superior and unique photophysical properties such as tunable emission wavelength, broad absorption spectra, narrow and symmetric emission spectra, high emission quantum yield and so on. These properties make QDs excellent energy donors in various fluorescence resonance energy transfer (FRET) processes [4, 5]. So far, the luminescent QD-FRET bioprobes have been widely utilized to detect a great variety of bio-related analytes including potassium ion [6], maltose [7], glucose [8], NADH [9], pH changing [10, 11], proteins [12, 13] and enzymes [14–17].

In addition, the QD-FRET bioprobes have also been widely used for the determination of DNA via DNA hybridization. The reported strategies for the construction of QD-DNA bioconjugates contain the streptavidin-biotin interaction [18, 19], electrostatic interaction [20, 21], amide bonding [22, 23] and metal-thiol bonding [24, 25]. Most of the reported streptavidin-biotin interaction and electrostatic interaction strategies required conjugation of streptavidin or some specific positive macromolecules to the surface of QDs, which increase the size of the complex at the detection system undoubtedly. Moreover, the reported amide bonding strategy required covalent conjugation of DNA to QD

surface by EDC/NHS coupling reaction that often decreases the stability and fluorescence intensity of QDs. These shortcomings can be overcome through metal-thiol bonding approach that represents a very simple method to efficiently bind DNA with QDs. These QD-DNA bioconjugates have better fluorescent properties and higher colloidal stability.

Hepatitis B virus (HBV) infection, which may cause some hepatic diseases including acute and chronic hepatitis, hepatocirrhosis, and liver cancer, is one of the major causes of death in the world and already becomes a huge health problem worldwide [26, 27]. Until now, some effective anti-HBV drugs have been developed to treat hepatic diseases by inhibiting viral replication [28, 29]. So, the determination of HBV DNA becomes much more important for the anti-HBV drugs exploitation and hepatic diseases therapy. Up to date, some approaches including real-time polymerase chain reaction (PCR) [30, 31], electrochemical detection [32, 33] and mass spectrometric analysis [34], have been reported to detect HBV DNA. However, some of these methods are expensive, complicated and time consuming for clinical diagnosis. Thus, there is an intense demand for simple and rapid sensor for HBV DNA determination with high sensitivity and specificity. In recent years, fluorescence analysis has been widely utilized for HBV DNA determination because of their unique advantages of simplicity, rapidity, high sensitivity and low cost of instrumentation and maintenance. Guan et al. have developed the fluorescent detection method for HBV DNA based on the fluorescent cationic polythiophene [35]. Nevertheless, some organic compounds have low quantum yield and low photostability, which could reduce the specificity and sensitivity of these methods.

Here, we established a simple and convenient assay of HBV DNA based on the luminescent QD-FRET bioprobe that composed of QD-DNA bioconjugates and ROX-DNA. The QD-DNA bioconjugates, the donors, were constructed through metal-thiol bonding. After adding 6-carboxy-X-rhodamine (ROX)-modified HBV DNA (ROX-DNA) into the QD-DNA bioconjugates solution, the DNA hybridization was formed and the FRET between QDs and ROX occurred. When unlabeled HBV DNA was added to occupy some hybridization sites firstly, the DNA hybridization between QD-DNA bioconjugates and ROX-DNA was inhibited partially and the FRET efficiency decreased (Fig. 1). The non-complementary DNA did not produce any variation of FRET signal because they could not inhibit the DNA hybridization between QD-DNA bioconjugates and ROX-DNA, which showed the convenient of the QD-FRET bioprobe. Based on these, the sensitive and specific determination of HBV DNA was achieved, which makes the procedure quite simple and rapid.

Experimental

Reagents

Selenium powder (Se, 99.99 %), stearic acid (98.5 %), hexadecylamine (HDA, 90 %), octadecene (ODE, 90 %), dioctylamine (DOA, 98 %), tributylphosphine (TBP, 97 %) and tri-n-octylphosphine oxide (TOPO, 90 %) were purchased from Sigma-Aldrich (St. Louis, MO, USA) and used as received. Sulfur (S), zinc acetate ($Zn(Ac)_2$), cadmium oxide (CdO) and mercaptoacetic acid (MAA) were purchased from Shanghai Reagent Factory (Shanghai, China). ROX was also purchased from Sigma-Aldrich (Milwaukee, WI, USA). All DNAs were purchased from Shanghai Sangon Biological Engineering Technology & Service Co., Ltd (Shanghai, China) and purified by HPLC. The sequences of these DNAs are listed in Table 1. All other reagents were of analytical-reagent grade and used as received from Sigma-Aldrich (St. Louis, MO, USA). Ultrapure water with a resistivity of 18.2 MΩ cm was produced by passing through a RiOs 8 unit followed by a Millipore-Q Academic purification set (Millipore, Bedford, MA, USA) and used throughout the whole experiments.

Apparatus

The absorption spectra were measured on a TU-1900 UV–vis spectrophotometer (Beijing Purkinje General Instrument Co., Ltd., Beijing, China). All fluorescence measurements were recorded with a Perkin-Elmer Model LS-55 luminescence spectrometer (PerkinElmer, Waltham, MA, USA) equipped with a 20 kW xenon discharge lamp as a light source. Quartz cells (1 cm path-length) were used for all measurements. The time-resolved fluorescence decay traces were recorded with a Fluorolog-3 system (Horiba Jobin Yvon, France) by using an excitation wavelength of 374 nm. The fluorescence images were recorded by the Nikon TE2000-U inverted fluorescence microscope with a Nikon INTENSILIGHT C-HGFI lamp, Q-IMAGING RETIGA 200R CCD and an oil-immersion objective (100 ×). The filter cube containing a 470±20 nm band-pass excitation filter, a 505 nm dichroic mirror, and a 520 nm barrier filter was used to ensure spectral purity. The agarose gel electrophoresis images were obtained by the ChemiDoc XRS (Bio-Rad, California, USA). All pH measurements were made with a basic pH meter PB-10 (Sartorius Scientific Instruments Co., Ltd., Beijing, China).

Preparation of MAA-QDs

The hydrophobic CdSe core QDs and CdSe/ZnS core/shell QDs were prepared according to the method described

Fig. 1 The principle of HBV DNA detection using the QD-FRET bioprobe. **a** When QDs were excited at 388 nm, fluorescence emission from ROX was induced through FRET between QDs donor and ROX acceptor in QD-FRET bioprobe. **b** and **c** No FRET was observed due to the displacement of ROX-DNA in the present of HBV DNA
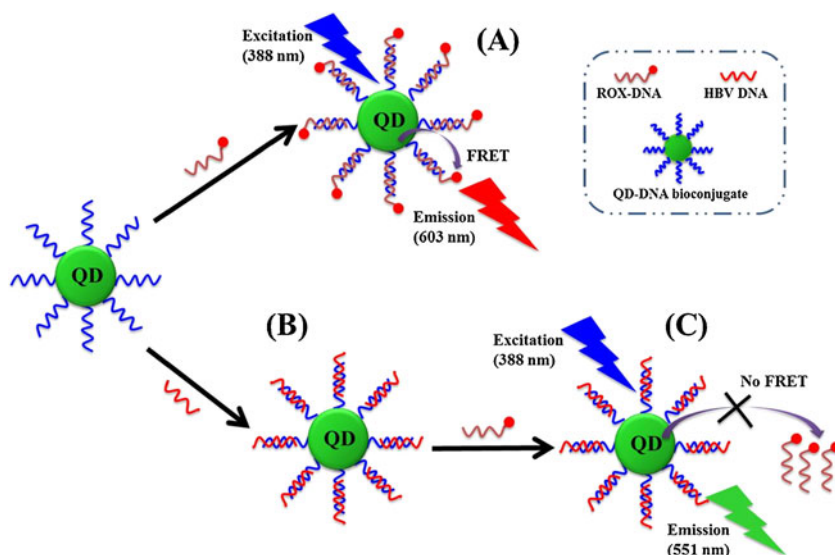
previously with little modification [36–38]. The water-soluble MAA-QDs were synthesized following the scheme described previously by surface ligand exchange [39, 40]. Briefly, the hydrophobic CdSe/ZnS QDs dispersed in hexane was first precipitated with acetone and then redispersed in chloroform. After that, MAA was added to chloroform/QDs solution and the mixture was stored at room temperature for 1 h. Finally, the mixture became opaque, which indicated the successful formation of MAA-QDs. The MAA-QDs were then centrifuged out at 10,000 rpm for 5 min. Afterward, ultrapure water was added to the pellet and pH was adjusted to 10–11 by dropwise addition of NaOH solution (1.0 mol L^{-1}). Next, acetone and water (50:50, v/v) was added to the aqueous solution to precipitate the MAA-QDs. The freshly prepared precipitate was dried in air and then redispersed in ultrapure water. The final MAA-QDs solution concentrations were estimated from the absorption spectra using the molar absorptivity at the first absorption maximum for QDs of this size [41]. The water-soluble MAA-QDs were quite stable under that storage conditions, with no changes in fluorescent property for 3 months.

Table 1 DNA sequences used in this report

DNAs	Sequences (5'-3')
Capture DNA	AAT ACC ACA TCA TCC ATA TA-(CH$_2$)$_6$-SH
ROX-DNA	ROX-TAT ATG GAT GAT GTG GTA TT
HBV DNA	TAT ATG GAT GAT GTG GTA TT
Non-complementary DNA	AAT ACC ACA TCA TCC ATA TA

Preparation and Characterization of QD-DNA Bioconjugates

The water-soluble MAA-QDs were dispersed in pH 7.2, 0.1 mol L^{-1} phosphate buffer with the final concentration of 1 μmol L^{-1}. Subsequently, the same solution containing 10 μmol L^{-1} capture DNA was added to the MAA-QDs solution and the mixed solution was then shaken gently at room temperature for 24 h. The mixture was further purified by using an ultra-filtration membrane (Microcon YM30, Millipore Corp., Bedford, MA, USA) according to the instructions from the manufacturer. The filtrate was collected and analyzed by UV–vis absorption. The amount of unconjugated capture DNA was calculated from the filtrate. Finally, the purified QD-DNA bioconjugates were dissolved in the ultrapure water and stored at 4 °C for further use. These QD-DNA bioconjugates were quite stable for at least 1 month with no noticeable precipitation or change in their fluorescence properties.

These QD-DNA bioconjugates were further characterized by mobility shift assay of the bioconjugates in agarose gel electrophoresis. Briefly, 10 μL of QD-DNA bioconjugates solution was loaded in 1.0 % agarose gel in Tris-acetate-ethylenediamine tetraacetic acid (TAE, 0.5 ×) buffer. As a control, 10 μL of MAA-QDs solution was loaded in another lane. After electrophoresis at 80 V for 30 min at 4 °C, the gel was illuminated and the digital images were captured by ChemiDoc XRS.

HBV DNA and Non-Complementary DNA Detection

As depicted in Scheme 1, firstly, 50 μL 10×DNA hybridization buffer (0.2 mol L^{-1} Tris–HCl, 5 mmol L^{-1} NaCl, pH 8.0), 7.5 μL 2.5 μmol L^{-1} QD-DNA bioconjugates solution

and the appropriate aliquot of the ROX-DNA solution were transferred into a 500 μL test tube. The mixture was stirred thoroughly and finally diluted to 500 μL with ultrapure water. After 30 min reaction at room temperature, the fluorescence spectra were measured to choose the appropriate ROX-DNA concentration.

For the HBV DNA detection, 50 μL 10×DNA hybridization buffer (0.2 mol L^{-1} Tris–HCl, 5 mmol L^{-1} NaCl, pH 8.0), 7.5 μL 2.5 μmol L^{-1} QD-DNA bioconjugates solution and the appropriate aliquot of the HBV DNA solution were transferred into a 500 μL test tube. The mixture was stirred thoroughly and finally diluted to 485 μL with ultrapure water. After 30 min reaction at room temperature, 15 μL 1.0 μmol L^{-1} ROX-DNA solution was added into the above mixture and the reaction lasted 30 min. After that, the fluorescence spectra were recorded to detect the HBV DNA. When the non-complementary DNA was determined, the HBV DNA solution was substituted by the non-complementary DNA solution.

The fluorescence spectra were recorded at excitation wavelength of 388 nm and the band-slits of both excitation and emission were set as 10.0 nm and 15.0 nm, respectively. The fluorescence spectra were recorded from 420 nm to 680 nm, the fluorescence intensity of QDs at 551 nm (I_d) and the fluorescence intensity of ROX at 603 nm (I_a) were used for quantitative analysis of the HBV DNA.

Results and Discussion

Characterization of QD-DNA Bioconjugates

The UV–vis absorption and fluorescence spectra of MAA-QDs and QD-DNA bioconjugates were all investigated (Fig. 2). It could be seen from the UV–vis absorption spectra that the first absorption maximums of MAA-QDs and QD-DNA bioconjugates were all at 522 nm, which indicated that the physical properties of QDs did not change after conjugating with the capture DNA. Meanwhile, the absorption value at 260 nm of QD-DNA bioconjugates did not change obviously (ΔA=0.003), which was due to the small amount of capture DNA on the surface of QDs. According to the amount of the unconjugated capture DNA calculated from the filtrate, we could speculate that the ratio of QDs to capture DNA was about 1 : 1.

With an excitation wavelength of 388 nm, QD-DNA bioconjugates exhibited an obvious, symmetrical fluorescence spectrum with an emission maximum at 551 nm without a tail on the right-hand side (Fig. 2). The fluorescence spectrum of QD-DNA bioconjugates was very narrow and the full width at half-maximum (FWHM) was about 30 nm. These results indicated that the as-prepared QD-
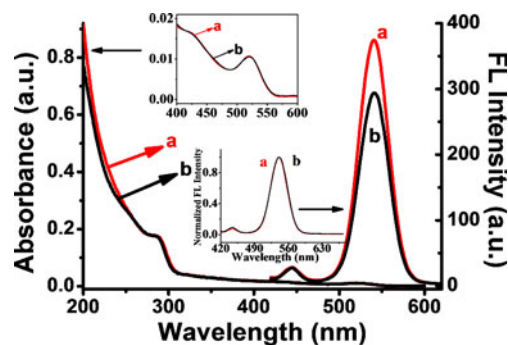

Fig. 2 The UV–vis absorption spectra and the fluorescence spectra of MAA-QDs (*a*) and QD-DNA bioconjugates (*b*). The insert were the UV–vis absorption spectra of MAA-QDs (*a*) and QD-DNA bioconjugates (*b*) from 400 nm to 600 nm, and the normalized fluorescence spectra of MAA-QDs (*a*) and QD-DNA bioconjugates (*b*) from 480 nm to 620 nm, respectively

DNA bioconjugates were nearly monodisperse and homogeneous as MAA-QDs alone. The optical properties of QDs were not influenced by capture DNA.

The fluorescence quantum yield (QY) of QD-DNA bioconjugates was also measured according to the method described by Crosby and his co-workers [42]. Fluorescein was chosen as the reference standard (QY 97 % in 0.1 mol L^{-1} NaOH solution). Then the fluorescence QY of QD-DNA bioconjugates could be calculated by comparing with the integrated areas of emission between fluorescein and QD-DNA bioconjugates. The experimental results supported that the fluorescence QY of QD-DNA bioconjugates was about 13 %, which was a little lower than that of MAA-QDs alone (15 %).

Furthermore, the mobility shift assay [24] was carried out to verify the successful conjugation between MAA-QDs and capture DNA by analyzing the change of the velocity of QDs after conjugation with capture DNA (Fig. 3). The more negatively charged QD-DNA bioconjugates migrated quicker than the negatively charged MAA-QDs, which further confirmed that the attachment of DNA to nanoparticles resulted in a change in the gel electrophoresis velocity of the nanoparticles [43]. When the running buffer, the strength of the electric field and the other conditions were the same, the charge-to-mass ratio of the material in the gel would determine the velocity. Due to the increase in the charge-to-mass ratio after the attachment of capture DNA to QDs, the QD-DNA bioconjugates ran quicker than MAA-QDs.

Spectral Properties of MAA-QDs and ROX

The FRET pair used in our work was composed of MAA-QDs as the donor and ROX as the acceptor. Figure 4 showed the normalized absorption spectra and the normalized fluorescence spectra of MAA-QDs and of ROX, respectively. As shown in Fig. 4, MAA-QDs showed a quite broad
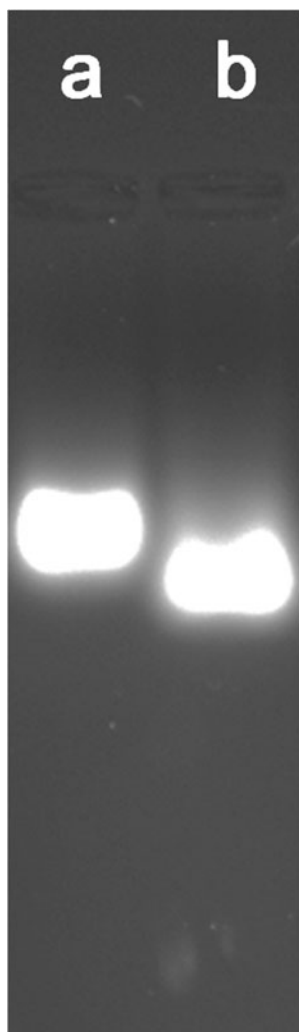
Fig. 3 Gel electrophoresis images of MAA-QDs (Lane **a**) and QD-DNA bioconjugates (Lane **b**)

absorption spectrum that allowed MAA-QDs to be excited using a near-UV wavelength (388 nm), which was far from the minimum of the absorption spectra of ROX. So, the direct excitation of ROX was efficiently minimized. Furthermore, MAA-QDs exhibited a narrow and symmetrical fluorescence spectrum with a maximum wavelength at 551 nm, which permitted minimal crosstalk between the donor and the acceptor emission spectra.

According to the Förster theory of FRET [44, 45], we could calculate the efficiency (E) of energy transfer between MAA-QDs (the donor) and ROX (the acceptor) by Eq. (1):

$$E = 1 - \frac{F}{F_0} = \frac{R_0^6}{R_0^6 + r^6} \tag{1}$$

Where r is the distance between the donor and the acceptor, and R_0 is the critical distance when the efficiency of

energy transfer is 50 %.

$$R_0^6 = 8.79 \times 10^{-25} K^2 N^{-4} \phi J \tag{2}$$

In Eq. (2), K^2 is the orientation factor related to the geometry of the donor and the acceptor of dipoles and $K^2=2/3$ for random orientation as in fluid solution; N is the refractive index of medium; ϕ is the quantum yield of the donor in the absence of the acceptor; J expresses the degree of spectral overlap between the donor emission spectrum and the acceptor absorption spectrum, which could be calculated by Eq. (3):

$$J = \frac{\int_0^\infty F(\lambda)\varepsilon(\lambda)\lambda^4 d\lambda}{\int_0^\infty F(\lambda)d\lambda} \tag{3}$$

Where, $F(\lambda)$ is the corrected fluorescence intensity of the donor in the wavelength range λ to $\lambda+\Delta\lambda$; $\varepsilon(\lambda)$ is the extinction coefficient of the acceptor at λ.

The overlap of the absorption spectra of ROX with the fluorescence spectra of MAA-QDs was also indicated in Fig. 4. In the present case, $N=1.33$, $\phi=0.151$, according to Eqs. (1) (3), we could calculate the Förster distance $R_0=2.77$ nm, and $r=2.37$ nm. The estimated R_0 in our FRET system was well in the range of typical Förster distance between 2 nm and 8 nm for the QDs(donor)-dye(acceptor) FRET systems [46, 47]. Since the absolute value of the average distance r was in the range of 2–8 nm [48] and the relationship between R_0 and r was $0.5R_0<r<1.5R_0$, the FRET between MAA-QDs to ROX would occur probably.

Furthermore, control experiments have been done between QD-DNA bioconjugates and ROX-DNA (Fig. 5). When the excitation wavelength was chosen at 388 nm, QDs showed strong fluorescence intensity at 551 nm in the solution with QD-DNA bioconjugates only and ROX exhibited almost no fluorescence emission at
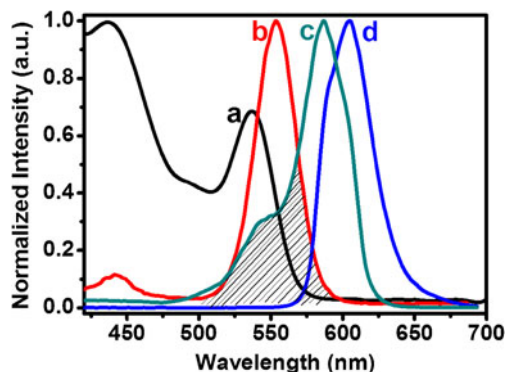

Fig. 4 The normalized absorption spectra of MAA-QDs (*a*) and ROX (*c*), and the normalized fluorescence spectra of MAA-QDs (*b*) and ROX (*d*)
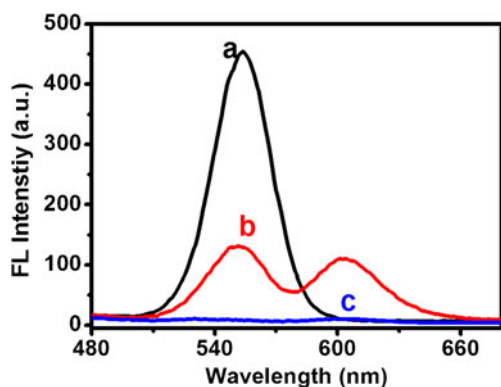
603 nm under direct excitation of ROX-DNA alone. However, when QD-DNA bioconjugates and ROX-DNA were mixed in the solution, two peaks at both 551 nm and 603 nm were observed due to the energy transfer from QDs to ROX. Through comparing the differences in the fluorescence intensities among different fluorescence spectra, the FRET occurrence between QDs and ROX could be further confirmed.

Detection of HBV DNA Based on QD-FRET Bioprobe

Since the detection of HBV DNA was performed by QD-FRET bioprobe, the QD-FRET bioprobe should be developed firstly. In order to construct QD-FRET bioprobe with high sensitivity and specificity, the influences of QD-DNA bioconjugates concentration and ROX-DNA concentration should be investigated first and foremost.

The preliminary experiment indicated that the hybridization reaction between QD-DNA bioconjugates and ROX-DNA was finished within 30 min in the DNA hybridization buffer, which contained 20 mmol L^{-1} Tris–HCl, pH 8.0 and 5 mmol L^{-1} NaCl. The fluorescence spectra of 37.5 nmol L^{-1} QD-DNA bioconjugates at different concentrations of ROX-DNA were recorded and the results were shown in Fig. 6a. After adding ROX-DNA into the DNA hybridization solution, the fluorescence intensity of QDs at 551 nm (I_d) decreased dramatically, meanwhile, the fluorescence intensity of ROX at 603 nm (I_a) increased significantly when excited at 388 nm. The hybridization of QD-DNA bioconjugates to ROX-DNA brought the ROX fluorophore spatially closer to the QDs [49], so the FRET efficiency between QDs and ROX was significantly improved. When the ROX-DNA concentration was increased from 0 to 30 nmol L^{-1}, the quenching efficiency of 37.5 nmol L^{-1} QD-DNA bioconjugates was raised from 0 to 62 % accordingly. Higher quenching efficiency did not occur with the increase
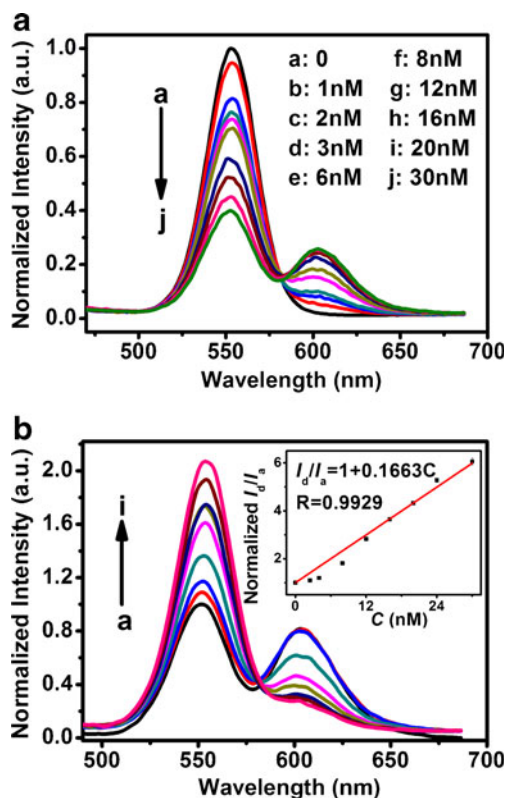
of ROX-DNA concentration, which resulted from the saturated hybridization between QD-DNA bioconjugates and ROX-DNA [50]. In order to enhance the sensitivity of HBV DNA determination, 37.5 nmol L^{-1} QD-DNA bioconjugates and 30 nmol L^{-1} ROX-DNA were chosen to develop the QD-FRET bioprobe.

Detection of HBV DNA using such QD-FRET bioprobe was carried out through displacement of ROX-DNA by HBV DNA in the DNA hybridization buffer. The initial experiments demonstrated that the hybridization of QD-DNA bioconjugates with HBV DNA was expeditious and completed in about 15 min at room temperature. So, after 30 min hybridization between QD-DNA bioconjugates and HBV DNA, ROX-DNA was added and then the mixture was further incubated for extra 30 min at the same conditions.

The fluorescence spectra of QD-FRET bioprobe at 0– 30 nmol L^{-1} HBV DNA were recorded and the corresponding spectra were shown in Fig. 6b. The experimental results

showed that the fluorescence intensity of QDs (I_d) increased steadily, while, the fluorescence intensity of ROX (I_a) decreased gradually with the increasing HBV DNA concentration. A linear relationship, between the normalized ratio I_d/I_a and the HBV DNA concentration, was also shown in the insert of Fig. 6b. The regression equation was $I_d/I_a = 1 + 0.1663 \times C$ (nmol L^{-1}) and the linear correlation coefficient was about 0.9929. The relative fluorescence intensity ratio (I_d/I_a) was normalized to (I_d/I_a)$_0$ that was the value of QD-FRET bioprobe without HBV DNA. The relative standard deviation (R.S.D.) for 12 nmol L^{-1} HBV DNA was 0.9 % ($n=5$). Based on the 3 times standard deviation of 8 measurements of QD-FRET bioprobe solution containing 20 nmol L^{-1} HBV DNA, the limit of HBV DNA detection was up to 1.5 nmol L^{-1} which could be comparable to the most sensitive method reported for HBV DNA detection [23].

In order to investigate the specificity of HBV DNA detection with our QD-FRET bioprobe, non-complementary DNA was chosen as control sequence under the same conditions. Since the non-complementary DNA could not hybridize with QD-DNA bioconjugates and could not inhibit the DNA hybridization reaction between QD-DNA bioconjugates and ROX-DNA, the fluorescence intensities of QDs and ROX were not affected obviously and the normalized ratio I_d/I_a
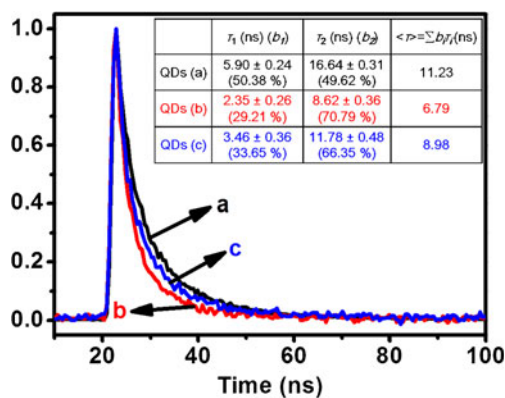

	τ_1 (ns) (b_1)	τ_2 (ns) (b_2)	$<\tau>=\sum b_i \tau_i$(ns)
QDs (a)	5.90 ± 0.24 (50.38 %)	16.64 ± 0.31 (49.62 %)	11.23
QDs (b)	2.35 ± 0.26 (29.21 %)	8.62 ± 0.36 (70.79 %)	6.79
QDs (c)	3.46 ± 0.36 (33.65 %)	11.78 ± 0.48 (66.35 %)	8.98

Fig. 7 The fluorescence decay traces of QD-DNA bioconjugates (*a*), QD-FRET bioprobe (*b*) and QD-FRET bioprobe reacted with 20 nmol L^{-1} HBV DNA (*c*) in the DNA hybridization buffer. All measurements were made at λ=551 nm. The concentrations of QD-DNA bioconjugates and ROX-DNA were 37.5 nmol L^{-1} and 30 nmol L^{-1}, respectively

was not changed either. These results validated the high specificity of QD-FRET bioprobe for HBV DNA testing. Meanwhile, the non-complementary DNA did not participate in FRET process, so it was unnecessary to remove such interferential DNAs. These suggested that such simple QD-FRET bioprobe was quite suitable for the high specific detection of HBV DNA.

Fig. 8 The digital fluorescence microscopy images of QD-DNA bioconjugates (**a**), QD-FRET bioprobe (**b**) and QD-FRET bioprobe for the monitoring of HBV DNA (**c**) and non-complementary DNA (**d**) in the DNA hybridization buffer. The concentrations of QD-DNA bioconjugates, ROX-DNA, HBV DNA and non-complementary DNA were 37.5 nmol L^{-1}, 30 nmol L^{-1}, 20 nmol L^{-1} and 20 nmol L^{-1}, respectively
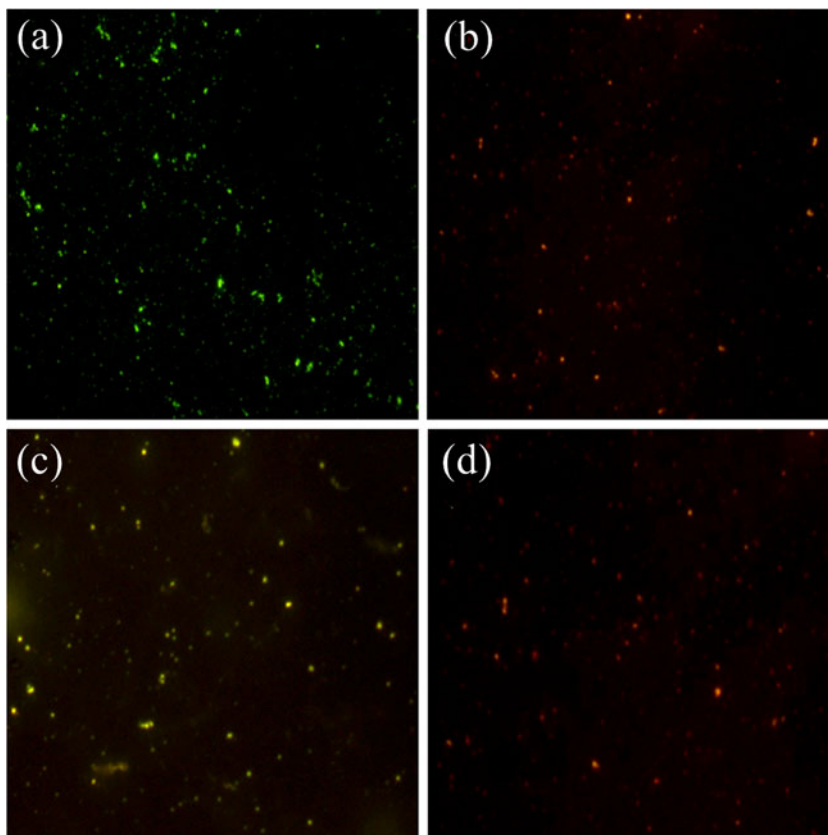
Time-Resolved Fluorescence Spectra of QD-FRET
Bioprobe–HBV DNA System

Furthermore, the time-resolved fluorescence spectra of QD-
FRET bioprobe–HBV DNA system were measured to char-
acterize the photophysical properties of this system. The
fluorescence decay curves of these systems were well fitted
with biexponential equation (see insert in Fig. 7). If the
intensity decays are multiexponential, it is important to use
an average decay time which is proportional to the
steadystate intensity [51, 52] and the amplitude weighted
lifetime are given by the sum of the $\Sigma b_i \tau_i$ products [53,
54]. As shown in Fig. 7, QD-DNA bioconjugates
exhibited two fluorescence decay components, τ_1 5.90
±0.24 ns (50.38 %) and τ_2 16.64±0.31 ns (49.62 %).
The corresponding average decay time of QD-DNA
bioconjugates was 11.23 ns. When the hybridization
interaction occured between QD-DNA bioconjugates
and ROX-DNA, two fluorescence decay components of
QD-DNA bioconjugates were shortened to τ_1 2.35±
0.26 ns (29.21 %) and τ_2 8.62±0.36 ns (70.79 %).
The average decay time of QD-DNA bioconjugates also
decreased to 6.79 ns. These results indicated the fluo-
rescence quenching of QDs by ROX and also confirmed
the occurrence of FRET between QDs and ROX. After
the treatment of the QD-FRET bioprobe with 20 nmol
L^{-1} HBV DNA, two fluorescence decay components of
QD-DNA bioconjugates increased to τ_1 3.46±0.36 ns
(33.65 %) and τ_2 11.78±0.48 ns (66.35 %). The QD-DNA
bioconjugates also recovered their original average decay time
partially, 8.98 ns, which was due to the incomplete displace-
ment of ROX-DNA by HBV DNA.

Fluorescence Images of QD-FRET Bioprobe–HBV DNA
System

Fluorescence images that simultaneously records the
QD-FRET bioprobe–HBV DNA system were carried
out by using Nikon inverted fluorescence microscope.
As shown in Fig. 8, the emission color of QD-DNA
bioconjugates was green (Fig. 8a) while that of QD-
FRET bioprobe was orange-red (Fig. 8b) in the DNA
hybridization buffer, which indicated the energy transfer
evidently from QDs donors to ROX acceptors. When
20 nmol L^{-1} HBV DNA was present in the QD-FRET
bioprobe solution, the emission color of the QD-DNA
bioprobe–HBV DNA system changed back to green
partially (Fig. 8c), which indicated the successful dis-
placement of ROX-DNA by HBV DNA in solution.
However, when 20 nmol L^{-1} non-complementary DNA
was added in QD-FRET bioprobe solution, the emission
color of this system was still orange-red (Fig. 8d),
which suggested the high specificity of HBV DNA

detection by our QD-FRET bioprobe. These experimen-
tal phenomena were consistent with the results reported
above. The experimental results showed the feasibility
of our QD-FRET bioprobe for the determination of
HBV DNA and for the distinction of HBV DNA by
fluorescence microscopy.

Conclusions

In summary, a simple and rapid method to detect HBV DNA
with high sensitivity and specificity based on the QD-FRET
bioprobe has been developed. The QD-FRET bioprobe was
composed of QD-DNA bioconjugates (donor) and ROX-
DNA (acceptor), which enabled the quantitative detection
of HBV DNA without the separation of non-complementary
DNA from hybridization system. Under the optimum con-
ditions, the method had a linear range of 2.5 – 30 nmol L^{-1}
with a 0.9929 correlation coefficient and the limit of HBV
DNA detection was 1.5 nmol L^{-1}, which demonstrated the
potential application prospects of this method for the high
throughput HBV DNA detection. Time-resolved fluores-
cence spectra and fluorescence images were further investi-
gated to verify the validity of the QD-FRET bioprobe and
observe the FRET phenomenon between QDs and ROX
successfully. This method enables a simple and efficient
detection that could be potentially used for other applica-
tions such as high throughput determinations of other dif-
ferent and specific DNA.

References

1. Bruchez M, Moronne M Jr, Gin P, Weiss S, Alivisatos AP (1998)
   Semiconductor nanocrystals as fluorescent biological labels.
   Science 281:2013–2016
2. Medintz IL, Uyeda HT, Goldman ER, Mattoussi H (2005)
   Quantum dot bioconjugates for imaging,labelling and sensing.
   Nat Mater 4:435–446
3. Huang S, Xiao Q, Li R, Guan HL, Liu J, Liu XR, He ZK, Liu Y
   (2009) A simple and sensitive method for L-Cysteine detection
   based on the fluorescence intensity increment of quantum dots.
   Anal Chim Acta 645:73–78
4. Huang S, Xiao Q, He ZK, Liu Y, Tinnefeld P, Su XR, Peng XN
   (2008) A high sensitive and specific QDs FRET bioprobe for
   MNase. Chem Commun 44:5990–5992
5. Qiu T, Zhao D, Zhou GH, Liang Y, He ZK, Liu ZH, Peng XN,
   Zhou L (2010) A positively charged QDs-based FRET probe for
   micrococcal nuclease detection. Analyst 135:2394–2399
6. Chen CY, Cheng CT, Lai CW, Wu PW, Wu KC, Chou PT, Chou
   YH, Chiu HT (2006) Potassium ion recognition by 15-crown-5
   functionalized CdSe/ZnS quantum dots in H2O. Chem Commun
   42:263–265

7. Medintz IL, Clapp AR, Mattoussi H, Goldman ER, Fisher B, Mauro JM (2003) Self-assembled nanoscale biosensors based on quantum dot FRET donors. Nat Mater 2:630–638

8. Tang B, Cao LH, Xu KH, Zhou LH, Ge JC, Li QL, Yu LJ (2008) A New Nanobiosensor for Glucose with High Sensitivity and Selectivity in Serum Based on Fluorescence Resonance Energy Transfer (FRET) between CdTe Quantum Dots and Au Nanoparticles. Chem Eur J 14:3637–3644

9. Freeman R, Gill R, Shweky I, Kotler M, Banin U, Willner I (2009) Biosensing and Probing of Intracellular Metabolic Pathways by NADH-Sensitive Quantum Dots. Angew Chem Int Ed 48:309–313

10. Tomasulo M, Yildiz I, Kaanumalle SL, Raymo FM (2006) pH-Sensitive Ligand for Luminescent Quantum Dots. Langmuir 22:10284–10290

11. Snee PT, Somers RC, Nair G, Zimmer JP, Bawendi MG, Nocera DG (2006) A Ratiometric CdSe/ZnS Nanocrystal pH Sensor. J Am Chem Soc 128:13320–13321

12. Levy M, Cater SF, Ellington AD (2005) Quantum-Dot Aptamer Beacons for the Detection of Proteins. ChemBioChem 6:2163–2166

13. Oh E, Hong MY, Lee D, Nam SH, Yoon HC, Kim HS (2005) Inhibition Assay of Biomolecules based on Fluorescence Resonance Energy Transfer (FRET) between Quantum Dots and Gold Nanoparticles. J Am Chem Soc 127:3270–3271

14. Xu CJ, Xing BG, Rao JH (2006) A self-assembled quantum dot probe for detecting β-lactamase activity. Biochem Biophys Res Commun 344:931–935

15. Chang E, Miller JS, Sun JT, Yu WW, Colvin VL, Drezek R, West JL (2005) Protease-activated quantum dot probes. Biochem Biophys Res Commun 334:1317–1321

16. Medintz IL, Clapp AR, Brunel FM, Tiefenbrunn T, Uyeda HT, Chang EL, Deschamps JR, Dawson PE, Mattoussi H (2006) Proteolytic activity monitored by fluorescence resonance energy transfer through quantum-dot-peptide conjugates. Nat Mater 5:581–589

17. Shi LF, Paoli VD, Rosenzweig N, Rosenzweig Z (2006) Synthesis and Application of Quantum Dots FRET-Based Protease Sensors. J Am Chem Soc 128:10378–10379

18. Zhang CY, Yeh HC, Kuroki MT, Wang TH (2005) Single-quantum-dot-based DNA nanosensor. Nat Mater 4:826–831

19. Zhang CY, Hu J (2010) Single Quantum Dot-Based Nanosensor for Multiple DNA Detection. Anal Chem 82:1921–1927

20. Peng H, Zhang LJ, Kjllman THM, Soeller C, Travas-Sejdic J (2007) DNA Hybridization Detection with Blue Luminescent Quantum Dots and Dye-Labeled Single-Stranded DNA. J Am Chem Soc 129:3048–3049

21. Jiang GX, Susha AS, Lutich AA, Stefani FD, Feldman J, Rogach AL (2010) Cascaded FRET in Conjugated Polymer/Quantum Dot/Dye-Labeled DNA Complexes for DNA Hybridization Detection (出版年为：2009年). ACSNANO 3:4127–4131

22. Algar WR, Krull UJ (2007) Towards multi-colour strategies for the detection of oligonucleotide hybridization using quantum dots as energy donors in fluorescence resonance energy transfer (FRET). Anal Chim Acta 581:193–201

23. Wang X, Lou XH, Wang Y, Guo QC, Fang Z, Zhong XH, Mao HJ, Jin QH, Wu L, Zhao H, Zhao JL (2010) QDs-DNA nanosensor for the detection of hepatitis B virus DNA and the single-base mutants. Biosens Bioelectron 25:1934–1940

24. Medintz IL, Berti L, Pons T, Grimes AF, English DS, Alessandrini A, Facci P, Mattoussi H (2007) A Reactive Peptidic Linker for Self-Assembling Hybrid Quantum Dot?DNA Bioconjugates. Nano Lett 7:1741–1748

25. Wu SM, Tian ZQ, Zhang ZL, Huang BH, Jiang P, Xie ZX, Pang DW (2010) Direct fluorescence in situ hybridization (FISH) in Escherichia coli with a target-specific quantum dot-based molecular beacon. Biosens Bioelectron 26:491–496

26. Mast EE, Alter MJ, Margolis HS (1999) Strategies to prevent and control hepatitis B and C virus infections: a global perspective. Vaccine 17:1730–1733

27. Malik AH, Lee WM (2000) Chronic hepatitis B virus infection: Treatment strategies for the next millennium. Ann Intern Med 132:723–731

28. Selabe SG, Song E, Burnett RJ, Mphahlele MJ (2009) Frequent detection of hepatitis B virus variants associated with lamivudine resistance in treated South African patients infected chronically with different HBV genotypes. J Med Virol 81:996–1001

29. Ntziora F, Parakevis D, Haida C, Magiorkinis E, Manesis E, Papatheodoridis G, Manolakopoulos S, Beloukas A, Chryssoy S, Magiorkinis G, Sypsa V, Hatzakis A (2009) Quantitative Detection of the M204V Hepatitis B Virus Minor Variants by Amplification Refractory Mutation System Real-Time PCR Combined with Molecular Beacon Technology. J Clin Microbiol 47:2544–2550

30. Hige S, Yamamoto Y, Yoshida S, Kobayashi T, Horimoto H, Yamamoto K, Sho T, Natsuizaka M, Nakanishi M, Chuma M, Asaka M (2010) Sensitive Assay for Quantification of Hepatitis B Virus Mutants by Use of a Minor Groove Binder Probe and Peptide Nucleic Acids. J Clin Microbiol 48:4487–4494

31. Xu GL, You QM, Pickerill S, Zhong HY, Wang HY, Shi J, Luo Y, You P, Kong HM, Lu FM, Hu L (2010) Application of PCR-LDR-nucleic acid detection strip in detection of YMDD mutation in hepatitis B patients treated with lamivudine. J Med Virol 82:1143–1149

32. Ye YK, Zhao JH, Yan F, Zhu YL, Ju XH (2003) Electrochemical behavior and detection of hepatitis B virus DNA PCR production at gold electrode. Biosens Bioelectron 18:1501–1508

33. Ariksoysal DO, Karadeniz H, Erdem A, Sengonul A, Sayiner AA, Ozsoz M (2005) Label-Free Electrochemical Hybridization Genosensor for the Detection of Hepatitis B Virus Genotype on the Development of Lamivudine Resistance. Anal Chem 77:4908–4917

34. Hong SP, Kim NK, Hwang SG, Chung HJ, Kim S, Han JH, Kim HT, Rim KS, Kang MS, Yoo W, Kim SO (2004) Detection of hepatitis B virus YMDD variants using mass spectrometric analysis of oligonucleotide fragments. J Hepatol 40:837–844

35. Guan HL, Cai M, Wang Y, He ZK (2010) Label-free DNA sensor based on fluorescent cationic polythiophene for the sensitive detection of hepatitis B virus oligonucleotides. Luminescence 25:311–316

36. Peng ZA, Peng XG (2001) Formation of high-quality CdTe, CdSe, and CdS nanocrystals using CdO as precursor. J Am Chem Soc 123:183–184

37. Zhou DJ, Bruckbauer A, Abell C, Klenerman D, Kang DJ (2005) Fabrication of Three-Dimensional Surface Structures with Highly Fluorescent Quantum Dots by Surface-Templated Layer-by-Layer Assembly. Adv Mater 17:1243–1248

38. Xiao Q, Huang S, Qi ZD, Zhou B, He ZK, Liu Y (2008) Conformation, thermodynamics and stoichiometry of HSA adsorbed to colloidal CdSe/ZnS quantum dots. BBA-Proteins Proteom 1784:1020–1027

39. Lei Y, Xiao Q, Huang S, Xu WS, Zhang Z, He ZK, Liu Y, Deng FJ (2011) Impact of CdSe/ZnS quantum dots on the development of zebrafish embryos. J Nanopart Res 13:6895–6906

40. Xiao Q, Zhou B, Huang S, Tian FF, Guan HL, Ge YS, Liu XR, He ZK, Liu Y (2009) Direct observation of the binding process between protein and quantum dots by in situ surface plasmon resonance measurements. Nanotechnology 20:325101

41. Yu WW, Qu LH, Guo WZ, Peng XG (2003) Experimental determination of the extinction coefficient of CdTe, CdSe, and CdS nanocrystals. Chem Mater 15:2854–2860

42. Crosby GA, Demas JN (1971) The measurement of photo-luminescence quantum yields. J Phys Chem 75:991–1024

43. Parak WJ, Gerion D, Zanchet D, Woerz AS, Pellegrino T, Micheel C, Williams SC, Seitz M, Bruehl RE, Bryant Z, Bustamante C, Bertozzi CR, Alivisatos AP (2002) Conjugation of DNA to Silanized Colloidal Semiconductor Nanocrystalline Quantum Dots. Chem Mater 14:2113–2119

44. Sklar LA, Hudson BS, Simoni RD (1977) Conjugated polyene fatty acids as fluorescent probes: synthetic phospholipid membrane studies. Biochemistry 16:819–828

45. Stryer L (1978) Fluorescence energy transfer as a spectroscopic ruler. Annu Rev Biochem 47:819–846

46. Lee SF, Osborne M (2007) Photodynamics of a Single Quantum Dot:? Fluorescence Activation, Enhancement, Intermittency, and Decay J Am Chem Soc 129:8936–8937

47. Pons T, Medintz IL, Wang X, English DS, Mattoussi H (2006) Solution-Phase Single Quantum Dot Fluorescence Resonance Energy Transfer. J Am Chem Soc 128:15324–15331

48. Valeur B, Brochon JC (1999) New trends in fluorescence spectroscopy. Springer Press, Berlin, p 25

49. Zhang CY, Johnson LW (2006) Quantum Dot-Based Fluorescence Resonance Energy Transfer with Improved FRET Efficiency in Capillary Flows. Anal Chem 78:5532–5537

50. Zhang CY, Johnson LW (2007) Microfluidic Control of Fluorescence Resonance Energy Transfer: Breaking the FRET Limit. Angew Chem Int Ed 46:3482–3485

51. Lakowicz JR (1999) Principles of fluorescence spectroscopy, 2nd edn. Kluwer Academic/Plenum Publishers, New York

52. Haldar KK, Sen T, Patra A (2010) Metal Conjugated Semiconductor Hybrid Nanoparticle-Based Fluorescence Resonance Energy Transfer. J Phys Chem C 114:4869–4874

53. Saini S, Srinivas G, Bagchi B (2009) Distance and Orientation Dependence of Excitation Energy Transfer: From Molecular Systems to Metal Nanoparticles. J Phys Chem B 113:1817–1832

54. Lee A, Coombs NA, Gourevich I, Kumacheva E, Scholes GD (2009) Lamellar Envelopes of Semiconductor Nanocrystals. J Am Chem Soc 131:10182–10188